Journal of Engineering Mathematics **29:** 347–369, 1995.

Numerical solutions of a damped Sine-Gordon equation in two space variables

K. DJIDJELI, W.G. PRICE and E.H. TWIZELL[1]
Department of Ship Science, University of Southampton, Southampton, England. SO9 5NH
[1] *Department of Mathematics and Statistics, Brunel University, Uxbridge, Middlesex, England. UB8 3PH (to whom all requests for off-prints should be addressed.) email: E.H. Twizell@brunel.ac.uk*

Received 30 September 1993; accepted in revised form 28 September 1994

Abstract. Numerical solutions of the perturbed Sine-Gordon equation in two space variables, arising from a Josephson junction are presented. The method proposed arises from a two-step, one parameter method for the numerical solution of second-order ordinary differential equations. Though implicit in nature, the method is applied explicitly. Global extrapolation in both space and time is used to improve the accuracy. The method is analysed with respect to stability criteria and numerical dispersion. Numerical results are obtained for various cases involving line and ring solitons.

1. Introduction

Over the last few years, it has become increasingly apparent that many physical phenomena in one space dimension can be described by a soliton model. Most of these models are based on simple integrable models such as the Sine-Gordon (SG) model, Korteweg-de Vries (KdV) equations and the nonlinear Schrodinger equation (NLS) [1, 2]. The soliton structures in these models are believed to be related to the integrability of the models themselves and the existence of an infinite number of conserved quantities is attributed to a remarkable stability of interacting solitons.

In recent years, some attention has also been paid to models which possess soliton-like structures in higher dimensions. In particular, the Josephson junction model [3] which consists of two layers of superconducting material separated by an isolating barrier. This model is found to have many applications in electronics and can be described by the two dimensional undamped Sine-Gordon equation. Moreover, it is found to possess soliton-like solutions [4].

Analytical solutions to the unperturbed Sine-Gordon equation with zero damping in higher dimensions have been obtained by Hirota [5], Lamb's method [6], Bäcklund transformation [7, 8] and Painlevé transcendents [9], while approximate solutions, chronologically, include those obtained by Christiansen and Lomdahl [4] and Argyris et al. [10]. The method proposed by Christiansen and Lomdahl was based on a generalized leapfrog method; and the development of the method by Argyris et al. was based on finite element techniques. Both methods have been applied successfully, for example, for the undamped Sine-Gordon equation in two space variables for a number of initial conditions, although in some particular cases, the finite element method appears to perform slightly better than the leapfrog method but at the cost of approximatively 25 times higher than the leapfrog method.

The presence of dissipative effects or other small perturbations can never be avoided in more realistic physical systems and lead also to equations too complicated to be integrated exactly. Thus, one may ask the basic question on how the soliton properties of the unperturbed Sine-Gordon equation in two space variables would be modified, if a perturbed term is added.

The perturbation considered here is a dissipative term and corresponds to a physically relevant effect in real Josephson junctions [11].

In this paper, the effect of the dissipative term in the solution of the Sine-Gordon equation in two space variables will be studied numerically. The method proposed is derived in Section 3 in which it is shown that the leapfrog method of Christiansen and Lomdahl [4] is in effect a special case (or a sub-scheme) of the proposed numerical method. The method is not expensive to implement, as the solution vector is obtained explicitly. In Section 4, the method is analysed with respect to stability criteria and numerical dispersion (the amplitude and phase errors of the method are analysed using a localized Fourier analysis). In Section 5, global extrapolation in both space and time is used to improve the accuracy of the method.

Numerical results obtained using this method for a sequence of initial conditions are reported in Section 6. The initial field distributions are chosen as kink profiles from one space dimension across lines or closed curves lying or moving in the xy-plane. Such waves will be denoted line and ring solitons respectively. In sub-section 6.2, superposition and perturbed line solitons as well as a moving-line soliton in inhomogeneous medium are investigated. Finally, the pulson behaviour of ring solitons in the case of a circular ring and the collision between non-concentric expanding ring solitons are also investigated.

The method developed is first tested on an equation for which the exact solution is known and then applied to an equation for which analytical results are not available at present.

2. The Associated System of Ordinary Differential Equations

Numerical solutions are sought to a Josephson junction which can be described by a damped Sine-Gordon equation in two space variables [11–12] given by

$$\frac{\partial^2 u}{\partial x^2} + \frac{\partial^2 u}{\partial y^2} - \frac{\partial^2 u}{\partial t^2} - \beta \frac{\partial u}{\partial t} = F(x, y) \sin u, \quad \beta \geqslant 0, \tag{2.1}$$

in the region $\Omega = \{(x, y), -a < x < a, -b < y < b\}$ for $t > 0$, where β is the dissipative term. The initial conditions are given at time $t = 0$ and are of the forms

$$u(x, y, 0) = f(x, y) \quad \text{and} \quad \frac{\partial u}{\partial t}(x, y, 0) = g(x, y)$$
$$-a \leqslant x \leqslant a, \quad -b \leqslant y \leqslant b. \tag{2.2}$$

The boundary conditions associated with (2.1) will be assumed to have the forms

$$\frac{\partial u}{\partial x} = p(x, y, t) \quad \text{for} \quad x = -a, \quad \text{and} \quad x = a, \quad -b < y < b, \quad t > 0, \tag{2.3}$$

$$\frac{\partial u}{\partial y} = q(x, y, t) \quad \text{for} \quad y = -b, \quad \text{and} \quad y = b, \quad -a < x < a, \quad t > 0, \tag{2.4}$$

where $p(x, y, t)$ and $q(x, y, t)$ are normal gradients along the boundary of the region Ω. The function $F(x, y)$ may be interpreted as a Josephson current density and $f(x, y)$ and $g(x, y)$ represent wave modes or kinks and velocity, respectively.

It may be noted that for $\beta = 0$, equation (2.1) reduces to the undamped Sine-Gordon equation in two space variables [4–10]. Some exact solutions of the undamped Sine-Gordon equation: $\partial^2 u/\partial x^2 + \partial^2 u/\partial y^2 - \partial^2 u/\partial t^2 = \sin u$ have been obtained (see [5–9]) but not to the damped Sine-Gordon equation (2.1), as far as the authors are aware.

The solution of (2.1) is sought in some region $R = \Omega \times [t > 0]$. The space intervals $-a \leqslant x \leqslant a$ and $-b \leqslant y \leqslant b$ are divided into $N+1$ subintervals each of width h_1 and h_2, respectively, so that $(N+1)h_1 = 2a$ and $(N+1)h_2 = 2b$, and the independent variable t will be discretized in steps of length l. At each time level $t = t_n = nl$ $(n = 0, 1, 2, \ldots)$ the rectangle Ω together with its boundary $\partial\Omega$ have been superimposed by a square mesh of $(N+2)^2$ points.

The solution $u(x, y, t)$ of (2.1) is sought at each point $(-a + kh_1, -b + mh_2, nl)$, where $k, m = 0, 1, 2, \ldots, N, N+1$ and $n = 0, 1, 2, \ldots$. The solution $u(-a + kh_1, -b + mh_2, nl)$ of (2.1) will be denoted by $u^n_{k,m}$, while the theoretical solution of an approximating difference scheme will be denoted by $U^n_{k,m}$ with

$$\begin{aligned}\mathbf{U}^n = (&U^n_{0,0}, U^n_{1,0}, \ldots, U^n_{N+1,0}; U^n_{0,1}, U^n_{1,1}, \ldots, U^n_{N+1,1}; \ldots; U^n_{0,N+1},\\ &U^n_{1,N+1}, \ldots, U^n_{N+1,N+1})^T,\end{aligned} \tag{2.5}$$

where T denotes transpose. Replacing the space derivatives in (2.1) by central difference approximants and applying the differential equation (2.1) to each of the discrete points $(-a + kh_1, -b + mh_2, nl)$ $(k, m = 0, 1, 2, \ldots, N+1$ and $n = 0, 1, 2, \ldots)$ at time level n, Eq. (2.1) is transformed into the second-order initial-value problem

$$\begin{aligned}&\frac{\mathrm{d}^2\mathbf{U}(t)}{\mathrm{d}t^2} + \beta\frac{\mathrm{d}\mathbf{U}(t)}{\mathrm{d}t} - A\mathbf{U}(t) + \mathbf{G}(\mathbf{U}(t)) - \mathbf{b}(t) = \mathbf{0}, \quad t > 0,\\ &\mathbf{U}(0) = \mathbf{f}, \frac{\mathrm{d}\mathbf{U}(0)}{\mathrm{d}t} = \mathbf{g},\end{aligned} \tag{2.6}$$

where $A = h_1^{-2}B + h_2^{-2}C$ is a matrix of order $(N+2)^2$ with B and C given by

$$B = \begin{pmatrix} B_1 & & & 0 \\ & \cdots & & \\ & & B_1 & \\ & & & \cdots \\ 0 & & & B_1 \end{pmatrix}, \text{ with } B_1 = \begin{pmatrix} -2 & 2 & & & \\ 1 & -2 & 1 & & \\ & \cdot & \cdot & \cdot & \\ & & \cdot & \cdot & \cdot \\ & & & 1 & -2 & 1 \\ & & & & 2 & -2 \end{pmatrix}. \tag{2.7}$$

and

$$C = \begin{pmatrix} -2I & 2I & & & & \\ I & -2I & I & & & \\ & \cdot & \cdot & \cdot & & \\ & & \cdot & \cdot & \cdot & \\ & & & I & -2I & I \\ & & & & 2I & -2I \end{pmatrix}, \tag{2.8}$$

where I is the identity matrix of order $N+2$. The matrix B is block diagonal with tridiagonal blocks and the matrix C is block tridiagonal with diagonal blocks. The vector $\mathbf{G}(\mathbf{U})$ is of order $(N+2)^2$ and is given by

$$\begin{aligned}\mathbf{G}(\mathbf{U}(t)) = (&F_{0,0}\sin U_{0,0}(t), F_{1,0}\sin U_{1,0}(t), \ldots, F_{N+1,0}\sin U_{N+1,0}(t);\\ &F_{0,1}\sin U_{0,1}(t), F_{1,1}\sin U_{1,1}(t), \ldots, F_{N+1,1}\sin U_{N+1,1}(t);\\ &\ldots\ldots\ldots; F_{0,N+1}\sin U_{0,N+1}(t), F_{1,N+1}\sin U_{1,N+1}(t),\\ &\ldots, F_{N+1,N+1}\sin U_{N+1,N+1}(t))^T,\end{aligned} \tag{2.9}$$

where $F_{k,m} = F(-a + kh_1, -b + mh_2)$ for $k, m = 0, 1, 2, \ldots, N, N+1$, and $\mathbf{b}(t) = \mathbf{b}_1(t) + \mathbf{b}_2(t)$ is a vector of boundary conditions with $\mathbf{b}_1(t)$ and $\mathbf{b}_2(t)$ given by

$$\begin{aligned}\mathbf{b}_1(t) = \frac{2}{h_1}(&- p(-a, -b, t), 0, \ldots, 0, p(a, -b, t); -p(-a, -b + h_2, t),\\ &0, \ldots, 0, p(a, -b + h_2, t); \ldots\ldots\ldots; p(-a, b, t),\\ &0, \ldots, 0, p(a, b, t))^T,\end{aligned} \tag{2.10}$$

and

$$\begin{aligned}\mathbf{b}_2(t) = \frac{2}{h_2}(&- q(-a, -b, t), -q(-a + h_1, -b, t), \ldots, -q(a, -b, t);\\ &0, \ldots\ldots\ldots, 0; q(-a, b, t), q(-a + h_1, b, t), \ldots, q(a, b, t))^T,\end{aligned} \tag{2.11}$$

respectively.

3. A Numerical Method

3.1. Development

Equation (2.6) can be transformed into a system of two equations, given by

$$\frac{\mathrm{d}\mathbf{U}(t)}{\mathrm{d}t} = -\beta\mathbf{U}(t) + \mathbf{V}(t), \quad t > 0, \quad \mathbf{U}(0) = \mathbf{f}, \tag{3.1}$$

and

$$\frac{\mathrm{d}\mathbf{V}(t)}{\mathrm{d}t} = A\mathbf{U}(t) + \mathbf{b}(t) - \mathbf{G}(\mathbf{U}(t)), \quad t > 0, \quad \mathbf{V}(0) = \mathbf{g}. \tag{3.2}$$

The numerical methods are based on the replacement of $\mathrm{d}\mathbf{U}(t)/\mathrm{d}t$, $\mathrm{d}\mathbf{V}(t)/\mathrm{d}t$ in (3.1) and (3.2) by the first-order forward difference approximants

$$\frac{\mathrm{d}\mathbf{U}(t)}{\mathrm{d}t} = \frac{\mathbf{U}(t + l) - \mathbf{U}(t)}{l} + O(l) \quad \text{as } l \to 0, \tag{3.3}$$

$$\frac{\mathrm{d}\mathbf{V}(t)}{\mathrm{d}t} = \frac{\mathbf{V}(t + l) - \mathbf{V}(t)}{l} + O(l) \quad \text{as } l \to 0, \tag{3.4}$$

where l is an increment in time (the time step). The solution of a numerical method at the point t_n will be denoted by $\mathbf{U}^n$ and $\mathbf{V}^n$ $(n = 0, 1, 2, \ldots)$.

Evaluating $\mathbf{U}$ on the right-hand side of (3.1) and (3.2) at $t = t_{n+1}$ and $t = t_n$ respectively and $\mathbf{V}$ in (3.1) at linear combination of $t = t_n$ and t_{n+1}, and then replacing $\mathrm{d}\mathbf{U}/\mathrm{d}t$ and $\mathrm{d}\mathbf{V}/\mathrm{d}t$ in (3.1) and (3.2) by (3.3) and (3.4) gives the implicit formula

$$\begin{cases}\mathbf{U}^{n+1} = \mathbf{U}^n - l\beta\mathbf{U}^{n+1} + \alpha l\mathbf{V}^n + (1 - \alpha)l\mathbf{V}^{n+1}, & (3.5)\\ \mathbf{V}^{n+1} = \mathbf{V}^n + l\left(A\mathbf{U}^n + \mathbf{b}^n - \mathbf{G}(\mathbf{U}^n)\right), & (3.6)\end{cases}$$

which, provided $1 + l\beta \neq 0$, may be rearranged to give a family of numerical methods

$$\begin{cases} \mathbf{U}^{n+1} = \dfrac{1}{1+l\beta}(\mathbf{U}^n + \alpha l\mathbf{V}^n + (1-\alpha)l\mathbf{V}^{n+1}), & (3.7) \\ \mathbf{V}^{n+1} = \mathbf{V}^n + l\,(A\mathbf{U}^n + \mathbf{b}^n - \mathbf{G}(\mathbf{U}^n))\,, & (3.8) \end{cases}$$

where α is some real parameter. Clearly, method $\{(3.7), (3.8)\}$ can be used explicitly by solving first (3.8) and then (3.7), though its derivation (formula (3.5)) classifies it to be implicit.

It is worth noting that $\{(3.8), (3.7)\}$ is a sequential algorithm for $\alpha \neq 1$ but, if $\alpha = 1$, $\mathbf{V}^{n+1}$ and $\mathbf{U}^{n+1}$ can be found simultaneously (i.e. in parallel) using a computer with two processors. Moreover, it can be seen also that by substituting $\mathbf{V}^{n+1}$ given by (3.8) into (3.7), the values of $\mathbf{U}^{n+1}$ and $\mathbf{V}^{n+1}$ can be found simultaneously, that is,

$$\begin{cases} \mathbf{W}^n = A\mathbf{U}^n, & (3.9) \\ \mathbf{U}^{n+1} = \dfrac{1}{1+l\beta}\left(\mathbf{U}^n + l\mathbf{V}^n + (1-\alpha)l^2(\mathbf{W}^n + \mathbf{b}^n - \mathbf{G}(\mathbf{U}^n))\right), & (3.10) \\ \mathbf{V}^{n+1} = \mathbf{V}^n + l(\mathbf{W}^n + \mathbf{b}^n - \mathbf{G}(\mathbf{U}^n)). & (3.11) \end{cases}$$

The algorithm (3.9)–(3.11) is well suited to parallel computation. The dominant calculation is the matrix-vector multiplication $A\mathbf{U}^n$ (the number of multiplications/divisions and additions/subtractions required to calculate the matrix-vector multiplication $A\mathbf{U}^n$ are $2(N+2)(4N+7)$ and $(N+2)(6N+7)$ respectively) which can be done in such a way that the components of $A\mathbf{U}^n$ can be calculated simultaneously using different processors. The calculated matrix-vector $A\mathbf{U}^n$ using different processors can then be used in equations (3.10) and (3.11) to find $\mathbf{U}^{n+1}$ and $\mathbf{V}^{n+1}$ simultaneously and thus the time needed to solve the PDE will be reduced significantly.

3.2. Leapfrog Scheme

Substituting equation (3.8) into (3.7), leads to

$$\mathbf{U}^{n+1} = \frac{1}{1+l\beta}[\mathbf{U}^n + l\mathbf{V}^n + (1-\alpha)l^2\{A\mathbf{U}^n + \mathbf{b}^n - \mathbf{G}(\mathbf{U}^n)\}]. \tag{3.12}$$

Writing, now, equation (3.12) at $n := n+1$, leads to

$$\mathbf{U}^{n+2} = \frac{1}{1+l\beta}[\mathbf{U}^{n+1} + l\mathbf{V}^{n+1} + (1-\alpha)l^2\{A\mathbf{U}^{n+1} + \mathbf{b}^{n+1} - \mathbf{G}(\mathbf{U}^{n+1})\}]. \tag{3.13}$$

Subtracting equation (3.12) from (3.13) gives

$$\begin{aligned} \mathbf{U}^{n+2} - \frac{1}{1+l\beta}\{&[(2+l\beta)I + (1-\alpha)l^2A]\mathbf{U}^{n+1} - (I - \alpha l^2A)\mathbf{U}^n \\ &+ l^2[(1-\alpha)\mathbf{b}^{n+1} + \alpha\mathbf{b}^n] - l^2[(1-\alpha)\mathbf{G}(\mathbf{U}^{n+1}) + \alpha\mathbf{G}(\mathbf{U}^n)]\} = \mathbf{0}. \end{aligned} \tag{3.14}$$

By replacing $\alpha = 0$, $\beta = 0$ and $n := n - 1$ in (3.14), equation (3.14) becomes

$$\mathbf{U}^{n+1} = (2I + l^2 A)\mathbf{U}^n - \mathbf{U}^{n-1} + l^2\mathbf{b}^n - l^2\mathbf{G}(\mathbf{U}^n). \tag{3.15}$$

It may be noted that method (3.15) is the leapfrog scheme used by Christiansen and Lomdahl [4]. In effect this is a sub-scheme (or special case) of the proposed general numerical method, which is shown in the next section, to have a wider range of application because of the flexibility in choosing the values of α and β.

4. Analysis of the Method

4.1. Local Truncation Error

The local truncation error of (3.14) at the point $u(x, y, t)$ is given by

$$\begin{aligned} L(x,y,t) \;=\; & \left(-\frac{\partial^3 u}{\partial t^3} - \frac{3}{2}\beta\frac{\partial^2 u}{\partial t^2} + (1-\alpha)\left(\frac{\partial^3 u}{\partial x^2 \partial t} + \frac{\partial^3 u}{\partial x^2 \partial t}\right)\right) l \\ & + \frac{1}{12}h_1^2\frac{\partial^4 u}{\partial x^4} + \frac{1}{12}h_2^2\frac{\partial^4 u}{\partial y^4} \\ & - (1-\alpha)F(x,y)(\sin u(x,y,t+l) - \sin u(x,y,t)). \end{aligned} \tag{4.1}$$

Differentiating equation (2.1) with respect to t and using the approximation $\sin u(x, y, t + l) = \sin u(x, y, t) + [u(x, y, t + l) - u(x, y, t)]\, \mathrm{d}\sin u/\mathrm{d}u$, equation (4.1) can be written as

$$\begin{aligned} L(x,y,t) \;=\; & -\left(\alpha\frac{\partial^3 u}{\partial t^3} + \left(\frac{1}{2}+\alpha\right)\beta\frac{\partial^2 u}{\partial t^2}\right) l \\ & + \frac{1}{12}h_1^2\frac{\partial^4 u}{\partial x^4} + \frac{1}{12}h_2^2\frac{\partial^4 u}{\partial y^4} + \cdots. \end{aligned} \tag{4.2}$$

Replacing, now, $h_2 = \frac{b}{a}h_1$ in equation (4.2), leads to

$$\begin{aligned} L(x,y,t) \;=\; & -\left(\alpha\frac{\partial^3 u}{\partial t^3} + \left(\frac{1}{2}+\alpha\right)\beta\frac{\partial^2 u}{\partial t^2}\right) l \\ & + \frac{1}{12}\left(\frac{\partial^4 u}{\partial x^4} + \frac{b^2}{a^2}\frac{\partial^4 u}{\partial y^4}\right) h_1^2 + \cdots. \end{aligned} \tag{4.3}$$

From this last equation, it is easy to see that the method {(3.7), (3.8)} is second-order in time when $\alpha\partial^3 u/\partial t^3 + (\frac{1}{2} + \alpha)\beta\partial^2 u/\partial t^2 = 0$ and first-order otherwise.

4.2. Stability Analysis and Dispersion Error

In an attempt to gain some insight into the stability of the method {(3.7), (3.8)}, linear stability theory is used for analysing the method. It is known that in the early stages an instability develops in a very small region. Therefore, if the solution is slowly varying, an instability may be predicted by means of a stability analysis of a localized version of the

difference scheme. That is, in the case of scheme (3.14), of the equation

$$\mathbf{U}^{n+2} = \frac{1}{1+l\beta}\Big\{[(2+l\beta)I + (1-\alpha)l^2A]\mathbf{U}^{n+1} - (I-\alpha l^2A)\mathbf{U}^n + l^2[(1-\alpha)\mathbf{b}^{n+1} + \alpha\mathbf{b}^n] - l^2G(\upsilon)\Big\}, \tag{4.4}$$

where $\upsilon = \max_{0<k,m<N+1}|U^0_{k,m}|$. In deriving Eq. (4.4), the vector $\mathbf{U}^n$ in $\mathbf{G}(\mathbf{U}^n)$, given by equation (2.9) is frozen (temporarily). However, although the application of the linear stability analysis to nonlinear equations cannot be rigorously justified it is found to be effective in practice (see for example, Greig and Morris [13] and Twizell et al. [14]).

Using Eq. (4.4), it follows that a perturbation $\mathbf{Z}^n = \mathbf{U}^n - \tilde{\mathbf{U}}^n$, where $\tilde{\mathbf{U}}^n$ is the computed solution, satisfies the equation

$$\mathbf{Z}^{n+2} = \left(\frac{(2+l\beta)I + (1-\alpha)l^2A}{1+l\beta}\right)\mathbf{Z}^{n+1} - \left(\frac{I-\alpha l^2A}{1+l\beta}\right)\mathbf{Z}^n. \tag{4.5}$$

This may be written as

$$\mathbf{E}^{n+2} = W\mathbf{E}^{n+1}, \tag{4.6}$$

or

$$\mathbf{E}^{n+1} = W\mathbf{E}^n, \tag{4.7}$$

where $\mathbf{E}^{n+1} = [(\mathbf{Z}^{n+1})^T, (Z^n)^T]^T$ and W is the amplification matrix given by

$$W = \begin{pmatrix} \dfrac{(2+l\beta)I + (1-\alpha)l^2A}{1+l\beta} & -\dfrac{(I-\alpha l^2A}{1+l\beta} \\ I & 0 \end{pmatrix}. \tag{4.8}$$

The global error in (4.7) will not grow as $n \to \infty$ if the eigenvalues of the amplification matrix W are less than unity in modulus. It is easy to see that the eigenvalues of W are given by the solution of the equation

$$\lambda^2 - \tau_1\lambda + \tau_2 = 0, \tag{4.9}$$

where $\tau_1 = (2 + l\beta + (1-\alpha)l^2\lambda_A)/(1+l\beta)$ and $\tau_2 = (1-\alpha l^2\lambda_A)/(1+l\beta)$. Using the Routh-Hurwitz criterion (see, for instance, Lambert [15]), the roots of (4.9) lie inside the unit circle if

$$1 + \tau_1 + \tau_2 > 0, \quad 1 - \tau_2 > 0, \quad \text{and} \quad 1 - \tau_1 + \tau_2 > 0, \tag{4.10}$$

Replacing τ_1 and τ_2 by their values in (4.10), leads to

$$\begin{cases} 4 + 2l\beta + (1-2\alpha)l^2\lambda_A > 0 & \text{(4.10a)} \\ -l^2\lambda_A > 0 & \text{(4.10b)} \\ \beta + \alpha l\lambda_A > 0 & \text{(4.10c)} \end{cases}$$

where λ_A is an eigenvalue of the matrix A. It can be shown that the $(N+2)^2$ eigenvalues of A are real and negative and are given by

$$\lambda_{k,m} = -4\left(h_1^{-2}\sin^2\frac{k\pi}{2(N+1)} + h_2^{-2}\sin^2\frac{m\pi}{2(N+1)}\right), \quad k, m = 0, 1, 2, \ldots, N+1. \tag{4.11}$$

From equation (4.10a), it follows that for $\alpha \geqslant \frac{1}{2}$, Eq. (4.10a) is true for all l and for $\alpha < \frac{1}{2}$, Eq. (4.10a) can be written as

$$4\frac{(1-2\alpha)l^2}{4+2l\beta}\left(h_1^{-2}\sin^2\frac{k\pi}{2(N+1)} + h_2^{-2}\sin^2\frac{m\pi}{2(N+1)}\right) < 1. \tag{4.12}$$

The maximum value of the left-hand side of (4.12) occurs when $\sin^2\frac{k\pi}{2(N+1)} = \sin^2\frac{m\pi}{2(N+1)} = 1$. Hence,

$$4\frac{(1-2\alpha)l^2}{4+2l\beta}(h_1^{-2} + h^{-2}) < 1, \tag{4.13}$$

that is,

$$l \leqslant \frac{\beta + \sqrt{\beta^2 + 16(1-2\alpha)\sigma}}{4(1-2\alpha)\sigma}, \tag{4.14}$$

where $\sigma = h_1^{-2} + h_2^{-2}$.

Turning next to equation (4.10b), is is easy to see that equation (4.10b) is true for all $\lambda_A < 0$. For the case $\lambda_A = 0$, the stability interval may be found by solving equation (4.9) directly. Substituting $\lambda_A = 0$ into Eq. (4.9), leads to

$$\lambda^2 - \frac{2+l\beta}{1+l\beta}\lambda + \frac{1}{1+l\beta} = 0. \tag{4.15}$$

The solutions of this equation are given by

$$\lambda_1 = 1, \quad \lambda_2 = \frac{1}{1+l\beta}. \tag{4.16}$$

From equation (4.16), it may be concluded that both solutions are less than or equal to unity for $\beta \geqslant 0$ and hence the method is stable.

Finally, turning to equation (4.10c), it can be seen that for $\alpha < 0$, Eq. (4.10c) is true for all $\lambda_A < 0$ and for $\alpha > 0$, Eq. (4.10c) can be written as

$$\frac{\beta}{\alpha l} + \lambda_A > 0. \tag{4.17}$$

For $\beta = 0$, (4.17) is not satisfied since $\lambda_A \leqslant 0$ and hence the method is unstable. For $\beta > 0$, it may be shown using (4.11) that

$$l \leqslant \frac{\beta}{4\alpha\sigma}. \tag{4.18}$$

Table 1 gives the range of values of α for which the method {(3.7), (3.8)} is stable.

Table 1. Stability of the method (3.7)–(3.8)

$\alpha \leqslant 0$	$0 < \alpha < \frac{1}{2}$	$\alpha \geqslant \frac{1}{2}$
Stable for $l \leqslant \dfrac{\beta + \sqrt{\beta^2 + 16(1-2\alpha)\sigma}}{4(1-2\alpha)\sigma}$	Stable for $l \leqslant \min\left(\dfrac{\beta + \sqrt{\beta^2 + 16(1-2\alpha)\sigma}}{4(1-\alpha)\sigma}, \dfrac{\beta}{4\alpha\sigma}\right)$ and $\beta > 0$ Unstable for $\beta = 0$	Stable for $l \leqslant \dfrac{\beta}{4\alpha\sigma}$ and $\beta > 0$ Unstable for $\beta = 0$

The physical model of the Sine-Gordon equation represents situations requiring large-scale time calculations. Thus, for wave simulations, the numerical method proposed should at least possess two properties. The first is that the method should represent faithfully amplitudes of the solution for many time steps and the second is that, since the positions of the wave fronts are as important as the amplitude of these waves, the proposed method should be capable of predicting such wave fronts with minimal error. Therefore, the phase error (dispersion) of the method must be small, over a long time calculation, since large phase errors can produce solutions that are totally out of phase with the (unknown) exact solution. That is, the method can produce solutions with exact amplitudes but with large errors in phase; a meaningless solution would then be obtained. In any discretization procedure only long waves can be approximated well. Thus, the amplitude and phase errors of the higher-frequency components are of little significance, and the main interest is in sufficiently small ξ and η.

The numerical phase of a method is defined as

$$P(\xi, \eta) = \tan^{-1}[\mathrm{Im}\{G(\xi, \eta)\}/\mathrm{Re}\{G(\xi, \eta)\}], \tag{4.19}$$

where ξ, η are the Fourier variables and $G(\xi, \eta)$ is the amplification factor (see Shokin [16] and Turkel [17]). By applying the von Neumann method to equation (4.4), it can be shown that the eigenvalues of the amplification matrix of Eq. (4.4) are given by

$$\{G(\xi, \eta)\}^2 - \frac{1}{1 + l\beta}\left((2 + l\beta) - 4(1-\alpha)l^2\mu\right) G(\xi, \eta) + \frac{1 + 4\alpha l^2\mu}{1 + l\beta} = 0, \tag{4.20}$$

where $\mu = h_1^{-2} \sin^2 \frac{1}{2}\xi + h_2^{-2} \sin^2 \frac{1}{2}\eta$ with $\xi = k_1 h_1$ and $\eta = k_2 h_2$; k_1 and k_2 are the wave numbers. It may be noted that the eigenvalues $G(\xi, \eta)$ of the equation (4.20) are the same as those given by equation (4.9); this may be seen just by substituting the eigenvalues λ_A of A given by (4.11) into (4.9).

The discriminant of equation (4.20) is given by

$$\Delta = \beta^2 - 16\mu - 8(1 + \alpha)\beta\mu l + 16(1 - \alpha)^2\mu^2 l^2. \tag{4.21}$$

For $\Delta < 0$, the solutions of equation (4.20) are given by

$$G(\xi, \eta) = \frac{1}{2(1 + \beta l)}\left((2 + l\beta) - 4(1 - \alpha)l^2\mu \pm il\sqrt{-\Delta}\right), \tag{4.22}$$

where $i = \sqrt{-1}$. Substituting Eq. (4.22) into Eq. (4.19) leads to

$$P(\xi, \eta) = \pm \tan^{-1}\left(\frac{l\sqrt{-\Delta}}{(2 + l\beta) - 4(1 - \alpha)l^2\mu}\right). \tag{4.23}$$

Define now $P_A(\xi,\eta) = l\omega(k_1,k_2)$ to be the analytic phase, where $\omega(k_1,k_2)$ is the dispersion relation. Then it can be shown that the dispersion relation for the equation (2.1) with constant coefficients, given by

$$\frac{\partial^2 u}{\partial x^2} + \frac{\partial^2 u}{\partial y^2} - \frac{\partial^2 u}{\partial t^2} - \beta\frac{\partial u}{\partial t} = F\sin v, \tag{4.24}$$

which can be reduced to

$$\frac{\partial^2 u}{\partial x^2} + \frac{\partial^2 u}{\partial y^2} - \frac{\partial^2 u}{\partial t^2} - \beta\frac{\partial u}{\partial t} = 0 \tag{4.25}$$

using the transformation $u(x,y,t) := u(x,y,t) + \frac{1}{4}(x^2+y^2)F\sin v$, satisfies the equation

$$\omega^2 + i\beta\omega - k_1^2 - k_2^2 = 0. \tag{4.26}$$

Solving this equation for ω gives the dispersion relation

$$\omega = \frac{1}{2}\left(-i\beta \pm \sqrt{-\beta^2 + 4(k_1^2+k_2^2)}\right). \tag{4.27}$$

Since $\mathrm{Im}\{\omega\} = -i\beta/2$, equation (4.27) is dissipative for $\beta > 0$ and unstable for $\beta < 0$ in which case the solution will grow without bound as time tends to infinity.

The numerical phase of (4.25) can also be shown to be given by (4.23). Thus, combining expressions (4.23) and (4.27) gives the following formula for the phase error (dispersion error)

$$E_\phi(\xi,\eta) = P(\xi,\eta) - P_A(\xi,\eta). \tag{4.28}$$

In the case $\beta = 0$, $P_A(\xi,\eta) = l\omega$ is real and so is $E_\phi(\xi,\eta)$ which is given by

$$E_\phi(\xi,\eta) = \pm\left(\tan^{-1}\left\{\frac{2l\sqrt{\mu[1-(1-\alpha)^2 l^2\mu]}}{1-2(1-\alpha)l^2\mu}\right\} - l\sqrt{h_1^{-2}\xi^2 + h_2^{-2}\eta^2}\right). \tag{4.29}$$

Equation (4.29) can also be used when $\beta \to 0$. For $E_\phi(\xi,\eta) > 0$, the numerical solution is said to be lagging behind the analytical solution.

Finally, it can be shown that the exact amplification factor of equation (4.25) is given by $\exp(-il\omega)$, where ω is given by the dispersion relation (4.26). Thus, the amplitude error is then given by

$$\begin{aligned} E_A(\xi,\eta) &= |G(\xi,\eta)| - |\exp(-il\omega)| \\ &= \sqrt{(1+\beta l)^{-1}(1+4\alpha l^2\mu)} - \sqrt{\exp\left(-\frac{1}{2}\beta l\right)} \end{aligned} \tag{4.30}$$

5. Global Extrapolation in Space and Time

The full global error at each grid-point at time T is given by the quantity E_1 (see (4.3)) which has the form

$$E_1 = le_1 + (e_2+e_3)h_1^2 + R_1, \tag{5.1}$$

in which $e_1 = -(\alpha\partial^3 u/\partial t^3 + (\frac{1}{2}+\alpha)\beta\partial^2 u/\partial t^2$, $e_2 = \frac{1}{12}\partial^4 u/\partial x^4$ and $e_3 = b^2/12a^2\,\partial^4 u/\partial y^4$ are independent of l, h_1 and T and the quantity R_1 is $O(l^{r^*} + h_1^{s^*})$ where $r^* > 1$ and $s^* > 2$ as $h_1 \to 0$ and $l \to 0$. Denoting by G_1 the grid characterized by h_1, $h_2 = h_1$ and l, the computation is repeated on a grid G_2 on which the space and time-steps are h_1, h_1 and $\frac{1}{2}l$, respectively. The full global error at time T is now given by

$$E_2 = 2^{-1}le_1 + h_1^2(e_2 + e_3) + R_2, \tag{5.2}$$

where $R_2 = O(l^{r^*} + h_1^{s^*})$. Suppose now that the computation is run a third time to time T on a grid G_3 characterized by $\frac{1}{2}h_1$, $\frac{1}{2}h_1$ and $\frac{1}{2}l$. The full global error at time T is now given by

$$E_3 = 2^{-1}le_1 + 2^{-2}h_1^2(e_2 + e_3) + R_3, \tag{5.3}$$

where $R_3 = O(l^{r^*} + h_1^{s^*})$. Considering the approximation $\mathbf{W}(T)$ given by

$$\mathbf{W}(T) = \alpha_1 \mathbf{I}_{\frac{h_1}{2},\frac{h_1}{2}} \mathbf{U}_{\frac{h_1}{2},\frac{h_1}{2},\frac{l}{2}} + \alpha_2 \mathbf{U}_{h_1,h_1,\frac{l}{2}} + (1 - \alpha_1 - \alpha_2)\mathbf{U}_{h_1,h_1,l}, \tag{5.4}$$

where the fine-to-coarse grid restriction operator $\mathbf{I}_{\frac{h_1}{2},\frac{h_1}{2}}$ isolates the $(N+2)^2$ elements of $\mathbf{U}_{\frac{h_1}{2},\frac{h_1}{2},\frac{l}{2}}$ corresponding to the $(N+2)^2$ elements of $\mathbf{U}_{h_1,h_1,\frac{l}{2}}$ and $\mathbf{U}_{h_1,h_1,l}$ ($\mathbf{U}_{\frac{h_1}{2},\frac{h_1}{2},\frac{l}{2}}$, $\mathbf{U}_{h_1,h_1,\frac{l}{2}}$ and $\mathbf{U}_{h_1,h_1,l}$ denote the solutions at time T on grid G_3, G_2 and G_1 and α_1 and α_2 are parameters) and the associated error

$$E_w = \alpha_1 E_3 + \alpha_2 E_2 + (1 - \alpha_1 - \alpha_2)E_1, \tag{5.5}$$

that is,

$$E_w = \left(1 - \frac{1}{2}(\alpha_1 + \alpha_2)\right) le_1 + \left(1 - \frac{3}{4}\alpha_1\right) h_1^2(e_2 + e_3) + R_w, \tag{5.6}$$

it may be shown that the terms in e_1, e_2 and e_3 vanish when

$$\alpha_1 = \frac{4}{3} \quad \text{and} \quad \alpha_2 = \frac{2}{3}. \tag{5.7}$$

This global extrapolation in both space and time using grids G_1, G_2 and G_3 has thus produced an approximation $\mathbf{W}(T)$ which is $O(l^{r^*} + h_1^{s^*})$ provided the parameters α_1 and α_2 take the values given in (5.7).

For $\alpha = 0$ and $\beta = 0$ respectively, it is easy to see from Eq. (5.1) that the method {(3.7), (3.8)} is second-order in both space and time, that is the full global error at each grid-point is given by

$$E_1 = l^2 e_4 + (e_2 + e_3)h_1^2 + R. \tag{5.8}$$

Using the same technique as before, it may be shown the new approximation $\mathbf{W}(T)$ is of order $O(l^{q^*} + h_1^{s^*})$, where $q^* > 2$ and $s^* > 2$ provided $\alpha_1 = \frac{4}{3}$ and $\alpha_2 = 0$.

6. Numerical Results

To observe the behaviour of the numerical method {(3.7), (3.8)}, it and its global extrapolation in time and space were tested on the following problem

$$\frac{\partial^2 u}{\partial x^2} + \frac{\partial^2 u}{\partial y^2} - \frac{\partial^2 u}{\partial t^2} - \beta\frac{\partial u}{\partial t} = \sin u, \quad -7 < x, y < 7, \quad t > 0, \tag{6.1}$$

with initial conditions

$$u(x, y, 0) = 4\tan^{-1}\left(\exp(x + y)\right), \quad -7 < x, y < 7, \tag{6.2}$$

$$\frac{\partial u}{\partial t}(x, y, 0) = -\frac{4\exp(x + y)}{1 + \exp(2x + 2y)}, \quad -7 \leqslant x, y \leqslant 7 \tag{6.3}$$

and boundary conditions

$$\frac{\partial u}{\partial x} = \frac{4\exp(x + y + t)}{\exp(2t) + \exp(2x + 2y)}$$
$$\text{for } x = -7 \text{ and } x = 7, \quad -7 < y < 7, \quad t > 0 \tag{6.4}$$

$$\frac{\partial u}{\partial y} = \frac{4\exp(x + y + t)}{\exp(2t) + \exp(2x + 2y)}$$
$$\text{for } y = -7 \text{ and } y = 7, \quad -7 < x < 7, \quad t > 0 \tag{6.5}$$

The theoretical solution of problem (6.1)–(6.5), in which the parameter β was given the value $\beta = 0$ is given by

$$u(x, y, t) = 4\tan^{-1}\left(\exp(x + y - t)\right). \tag{6.6}$$

The solution was computed for x and y in the intervals $-7 \leqslant x, y \leqslant 7$ and $t > 0$. The space and time steps, h and l, were given the values (i) $h = 0.25$ and $l = 0.1$ and (ii) $h = 0.1$ and $l = 0.05$. The errors in the L_2 and L_∞ norms at time $t = 1$, 3, 5 and 7 using method {(3.7), (3.8)} and its extrapolation are given in Table 2 for different values of α. It can be seen from these values that for $\beta = 0$ the method is stable when $\alpha \leqslant 0$ and the condition (4.14) is satisfied, and unstable when $\alpha > 0$. These results agree with the theory given in Section 4. Furthermore, it is easy to see that the extrapolation procedure involving both space and time produced noticeable reductions in error when $\alpha < 0$ but at the cost of significantly increasing the computation time (one way to speed up calculations is to use the algorithm in parallel). By decreasing the space and the time steps ($h = 0.1$ and $l = 0.05$), it was found that the errors given by the method (3.7)–(3.8) and its extrapolation have been only slightly improved in comparison with those given for $l = 0.25$ and $l = 0.1$.

The results for $\alpha = 0$ in Table 2 correspond to those given by the leapfrog scheme used by Christiansen and Lomdahl [4]. It can be seen from this table that the errors given by the method (3.7)–(3.8) for $\alpha = 0$ are similar to those given by this method for $\alpha = -0.01$. The errors associated with the space-time extrapolation for $\alpha = 0$ are not reflected however in Table 2 as desired.

In Tables 3 and 4, the analytic phase and the modulus of the exact amplification factor together with the numerical phase (4.23) and the modulus of the numerical amplification factor $G(\xi, \eta)$ (4.22) are compared for the values of $h = 0.25$ and $l = 0.1$ for the case $\xi = \eta$ only (mainly chosen to avoid displaying all other results corresponding to other values of ξ and η ($\xi \neq \eta$) as they require too much space). It can be seen from Table 3 that the difference between the analytic and the numerical phases are small. The same thing can also be noticed for the amplitude (see Table 4). Moreover, as $|G(\xi, \eta)| \approx 1$, the method (3.7)–(3.8) is nearly nondissipative. By choosing different values of the space and time steps, within the scheme's

Table 2. Error norms at $t = 1, 3, 5$ and 7 using the explicit method (3.7)–(3.8) with $\beta = 0$, $\alpha = -0.01, 0, 0.2$ and 0.5.

			Method (3.7)–(3.8)				Space-time extrapolation		
α	h	l	t	L_2	L_∞	CPU(s)	L_2	L_∞	CPU(s)
−0.01	0.25	0.1	1.0	0.7339	0.0354	0.40	0.0128	0.0013	4.38
			3.0	0.7849	0.0392	1.49	0.0339	0.0037	10.98
			5.0	0.4971	0.0464	1.65	0.0653	0.0058	17.39
			7.0	0.6817	0.0355	2.20	0.0932	0.0099	23.64
0.0	0.25	0.1	1.0	0.7221	0.0350	0.70	0.2595	0.0276	6.05
			3.0	0.7877	0.0431	1.47	0.3186	0.0177	13.39
			5.0	0.5167	0.0404	2.12	0.2731	0.0205	20.91
			7.0	0.6531	0.0353	2.79	0.3237	0.0323	27.56
0.2	0.25	0.1	1.0	0.5180	0.0258	0.70	0.0076	0.0016	6.05
			3.0	1.0138	0.0758	1.47	0.0316	0.0033	13.39
			5.0	1.7096	0.1752	2.12	0.1263	0.0198	20.91
			7.0	3.1385	0.3615	2.79	2.7906	0.4437	27.56
0.5	0.25	0.1	1.0	0.4896	0.0350	0.70	0.0236	0.0039	6.05
			3.0	1.7834	0.1942	1.47	1.4776	0.4884	13.39
			5.0	7.8200	1.1874	2.12	12607.768	2936.244	20.91
			7.0	825.215	192.877	2.79	–	–	27.56

Table 3. Analytic and Numerical Phase for $h = 0.25, l = 0.1, \alpha = -0.01$ and $\beta = 0$.

ξ	Analytic Phase	Numerical Phase
0.000	0.000	0.000
0.100	0.057	0.057
0.200	0.113	0.113
0.300	0.170	0.169
0.400	0.226	0.225
0.500	0.283	0.281
0.600	0.339	0.336
0.700	0.396	0.391
0.800	0.453	0.445
0.900	0.509	0.498
1.000	0.566	0.550

Table 4. Amplitude Errors for $h = 0.25, l = 0.1, \alpha = -0.01$ and $\beta = 0$.

ξ	$\lvert\exp(-il\omega)\rvert$	$\lvert G(\xi,\eta)\rvert$
0.000	1.0000	1.0000
0.100	1.0000	1.0000
0.200	1.0000	0.9999
0.300	1.0000	0.9999
0.400	1.0000	0.9997
0.500	1.0000	0.9996
0.600	1.0000	0.9994
0.700	1.0000	0.9992
0.800	1.0000	0.9990
0.900	1.0000	0.9988
1.000	1.0000	0.9985

stability range, the method was found to offer a good phase representation. It also appears that the larger the ratio $r = l/h$ one uses, within the scheme's stability range, the smaller the phase error.

Note, the analytic and numerical phases given in Table 3 correspond only to those given by the equations with positive sign (see (4.23) and (4.27)). The other results of the analytical and numerical phases which correspond to the negative sign can be found simply by multiplying the values given in Table 3 by (-1).

All the calculations were performed on a Sun SPARC station 10 using Fortran with double precision arithmetic and the plots in all figures were obtained using the graphical system Unimap 2000.

In the numerical calculations that follow, various cases involving line and ring solitons for the solution of (2.1) are reported; the parameters α and β were given the values $\alpha = -0.01$ and $\beta = 0.05$ and the extrapolation method was used. In all the following experiments, the boundary conditions are taken to be

$$\frac{\partial u}{\partial x} = 0 \quad \text{and} \quad \frac{\partial u}{\partial y} = 0 \tag{6.7}$$

6.1. Energy Conservation

The existence of conservation laws has been shown to be a characteristic property of soliton-producing equations. Thus, the conserved quantities may be used to provide a check on numerical integrations. It is desired therefore, to establish such a quantity which is conserved with respect to time t for the Sine-Gordon equation. Multiplying equation (2.1) by u_t and integrating over the x–y region yields

$$\int\int [u_t u_{tt} + \beta u_t^2 - u_t(u_{xx} + u_{yy}) + F u_t \sin u]\mathrm{d}x\mathrm{d}y = 0. \tag{6.8}$$

By integrating by parts and then using the boundary conditions (6.7), equation (6.8) can be reduced to

$$\frac{\partial}{\partial t}\left\{\frac{1}{2}\int\int [u_x^2 + u_y^2 + u_t^2 + 2(1 - \cos u)]\mathrm{d}x\mathrm{d}y\right\} = -\beta\int\int (u_t)^2\mathrm{d}x\mathrm{d}y. \tag{6.9}$$

For $\beta = 0$, the energy for the undamped Sine-Gordon equation given by

$$E = \frac{1}{2}\int\int [u_x^2 + u_y^2 + u_t^2 + 2(1 - \cos u)]\mathrm{d}x\mathrm{d}y, \tag{6.10}$$

is conserved, while for $\beta > 0$, the energy is not conserved; this term indicates the energy dissipated from the wave system.

6.2. Line Solitons

6.2.1. Superposition of two line solitons

The superposition of two line solitons is obtained for $F(x, y) = 1$ and initial conditions

$$f(x, y) = 4\tan^{-1}\exp(x) + 4\tan^{-1}\exp(y), \quad -6 \leqslant x, y \leqslant 6, \tag{6.11}$$

$$g(x, y) = 0, \quad -6 \leqslant x, y \leqslant 6 \tag{6.12}$$

and are presented in Fig. 1 for $\beta = 0.05$. The numerical solutions at times $t = 1$, 2, 3 and 4 are also shown. The results in Fig. 1 show the break up of two orthogonal line solitons which move away from each other undisturbed. For a small value of β, the dissipative term is found to have little effect on the superposition of two line solitons, although at time $t = 4$, its effect started to become visible as the moving of the break up of two orthogonal line solitons has slowed down in comparison with the undamped case. For a large value of β, however, the

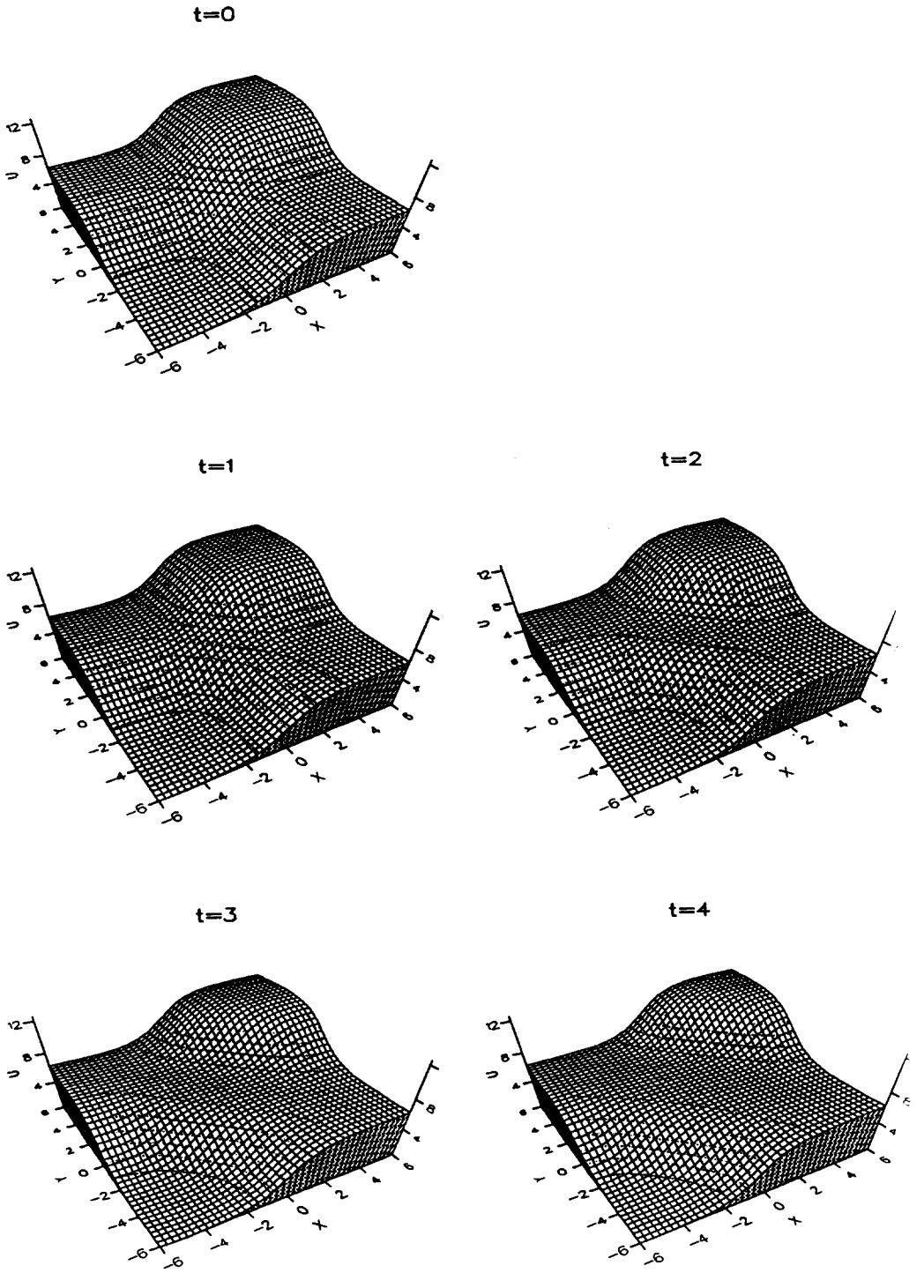

Fig. 1.

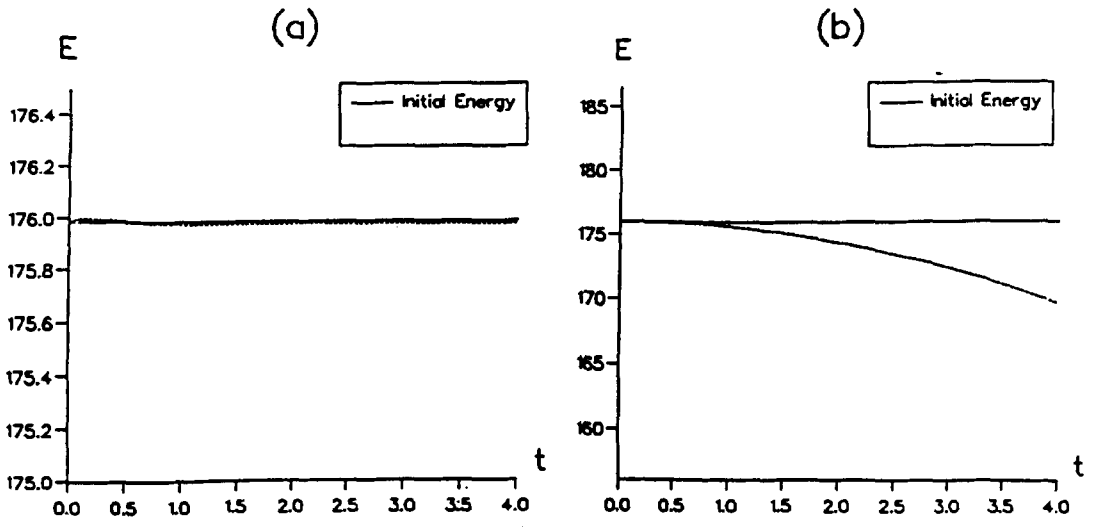

Fig. 2.

dissipative term is found to slow down the separation and break up of two orthogonal line solitons as time increases. The CPU time required to reach $t = 4$ was 8.96 seconds using the space-time extrapolation method.

A numerical check of the conservation of energy in the case of the undamped/damped Sine-Gordon equation is given. The resulting energy is shown in Figure 2(a) for $0 < t \leqslant 4$. It can be seen from this figure that for $\beta = 0$ (undamped Sine-Gordon equation), the energy remains constant as time increases, while for $\beta = 0.05$, the energy is found to be decreasing as time increases (see Figure 2(b)); this is due to the dissipative term.

The initial energy ($t = 0$) is obtained over the region Ω by insertion of the initial conditions (6.11) and (6.12) into equation (6.10) and is given by

$$
\begin{aligned}
E_{Initial} = {} & 8\left(\frac{b[\exp(a)-\exp(-a)]}{\exp(a)+\exp(-a)} + \frac{a[\exp(b)-\exp(-b)]}{\exp(b)+\exp(-b)}\right) \\
& +8\left(\frac{1}{1+\exp(-2a)} - \frac{1}{1+\exp(2a)}\right) \\
& \times\left(\frac{1}{1+\exp(2b)} - \frac{1}{1+\exp(-2b)} + b\right) \\
& +8\left(\frac{1}{1+\exp(-2b)} - \frac{1}{1+\exp(2b)}\right) \\
& \times\left(\frac{1}{1+\exp(2a)} - \frac{1}{1+\exp(-2a)} + a\right) \\
& +4[\sin 2\tan^{-1}(\exp a) - \sin 2\tan^{-1}(\exp(-a))] \\
& \times[\sin 2\tan^{-1}(\exp b) - \sin 2\tan^{-1}(\exp(-b))].
\end{aligned}
$$

The energies given in Fig. 2 are obtained as a linear combination of the three energies given on the grids G_1, G_2 and G_3 using the composite trapezoidal rule for integration, that is, $E = \frac{4}{3}E_{G_1} + \frac{2}{3}E_{G_2} - E_{G_3}$, where E_{G_1}, E_{G_2} and E_{G_3} are the energies obtained on the grids G_1, G_2 and G_3 respectively.

6.2.2. Perturbation of a line soliton

Perturbation of a single soliton has been depicted in Fig. 3 for $\beta = 0.05$ in terms of $\sin(u/2)$ at $t = 2, 3, 5, 7$ and 11. These results are for the case $F(x, y) = 1$ and initial conditions

$$f(x,y) = 4\tan^{-1}\exp(x + 1 - 2\text{sech}(y + 7) - 2\text{sech}(y - 7)),$$
$$-7 \leqslant x, y \leqslant 7, \tag{6.13}$$
$$g(x,y) = 0 \quad -7 \leqslant x, y \leqslant 7. \tag{6.14}$$

The results show two symmetric dents moving towards each other, interacting at time $t = 7$ and after interaction the dents are seen to retain their shape after the collision. As before, a small dissipative term is found to have little effect on the symmetric perturbation of static line solitons but a large dissipative term β is found to slow down the formation of the dents.

6.2.3. Line soliton in an inhomogeneous medium

Numerical solutions for a line soliton in an inhomogeneous medium are obtained for the Josephson current density $F(x, y) = 1 + \text{sech}^2\sqrt{x^2 + y^2}$ and the initial conditions

$$f(x,y) = 4\tan^{-1}\exp\left((x - 3.5)/0.954\right), \quad -7 \leqslant x, y \leqslant 7 \tag{6.15}$$
$$g(x,y) = 0.629\text{sech}\left((x - 3.5)/0.954\right), \quad -7 \leqslant x, y \leqslant 7 \tag{6.16}$$

and are presented in Fig. 4 for $\beta = 0.05$ in terms of $\sin(u/2)$ at $t = 6$, 12 and 18 in the region $-7 \leqslant x, y \leqslant 7$. The results in Fig. 4 show that the line soliton is moving almost as a straight line during the transmission through inhomogeneity. For a large value of β, transmission of the line soliton across inhomogeneity was found to hardly move the soliton from its initial position ($t = 0$), the dissipative term is slowing down the evolution of the line soliton as time increases.

6.3. Ring Solitons

6.3.1. Circular ring soliton

Circular ring solitons are found for the case $F(x, y) = 1$ and initial conditions

$$f(x,y) = 4\tan^{-1}\exp(3 - \sqrt{x^2 + y^2}), -7 \leqslant x, y \leqslant 7 \tag{6.17}$$
$$g(x,y) = 0 \qquad -7 \leqslant x, y \leqslant 7. \tag{6.18}$$

The solutions were sought over the domain $-7 \leqslant x, y \leqslant 7$ and are presented in Fig. 5 for $\beta = 0.05$ at $t = 2.8$, 5.6, 8.4, and 11.2 in terms of $\sin(u/2)$. At the initial stage ($t = 0$), it can be seen that the ring soliton shrinks and as time goes on, oscillations and radiations begin to form and continue to form up to $t = 8.4$. At $t = 11.2$, the graph shows that a ring soliton is nearly formed again (in the case of the damping switched off, the ring soliton was found to be already formed). For a large value of β, the initial shrunk ring soliton was found to be changing very slowly from its initial position as time increases.

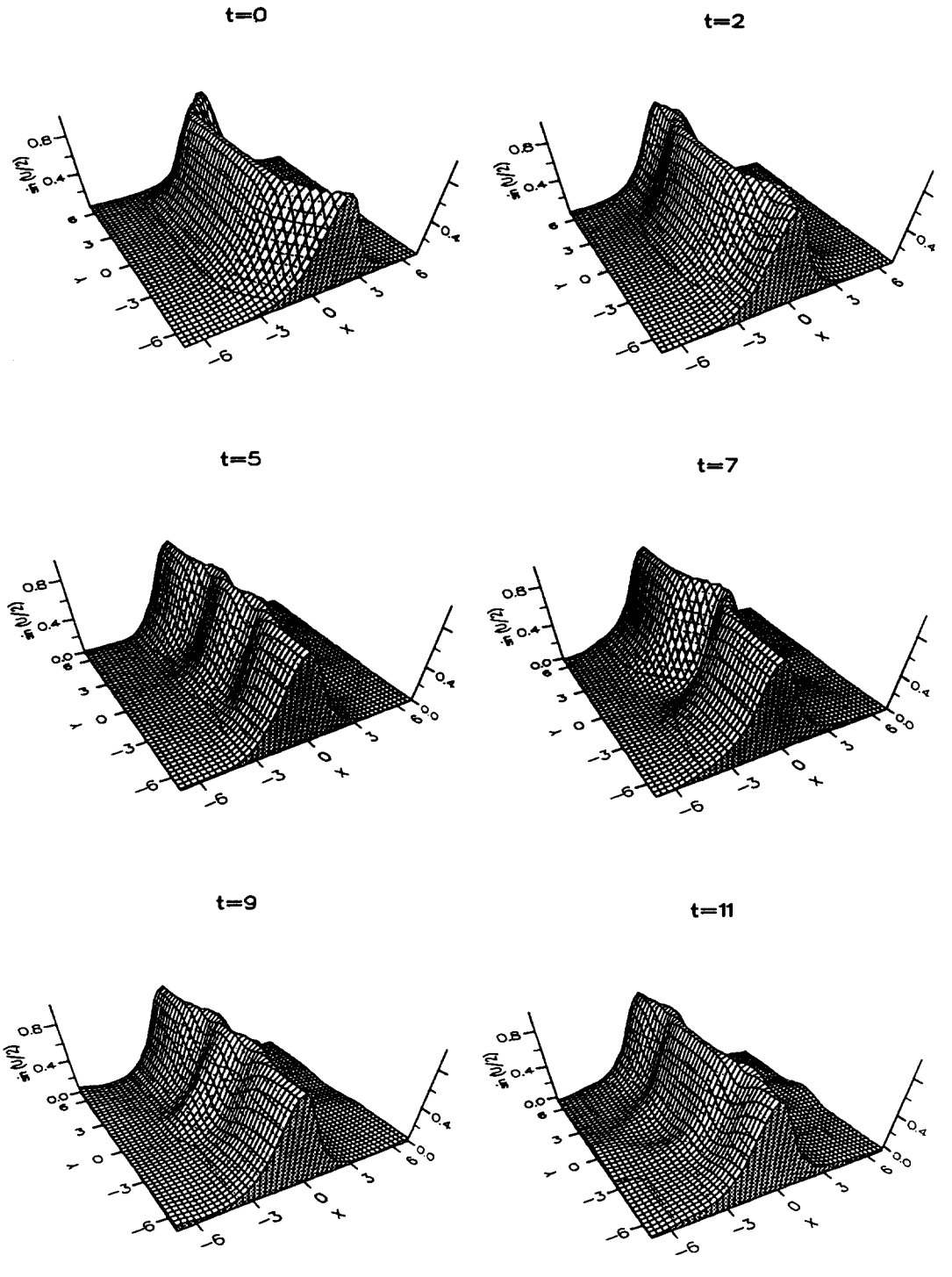

Fig. 3.

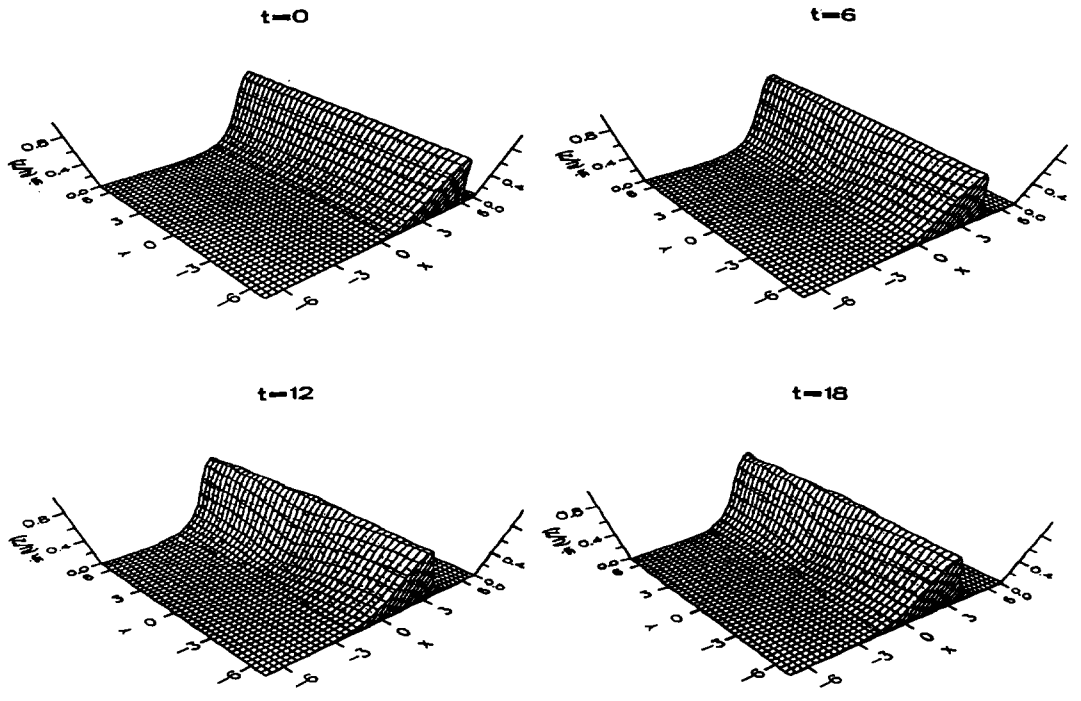

Fig. 4.

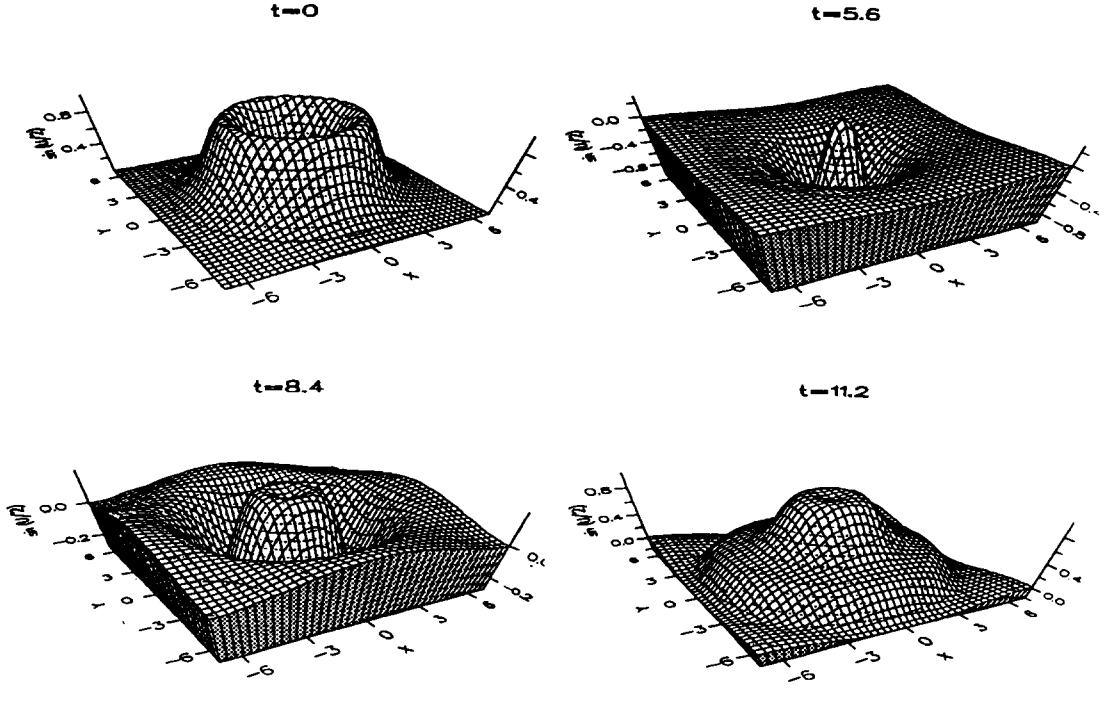

Fig. 5.

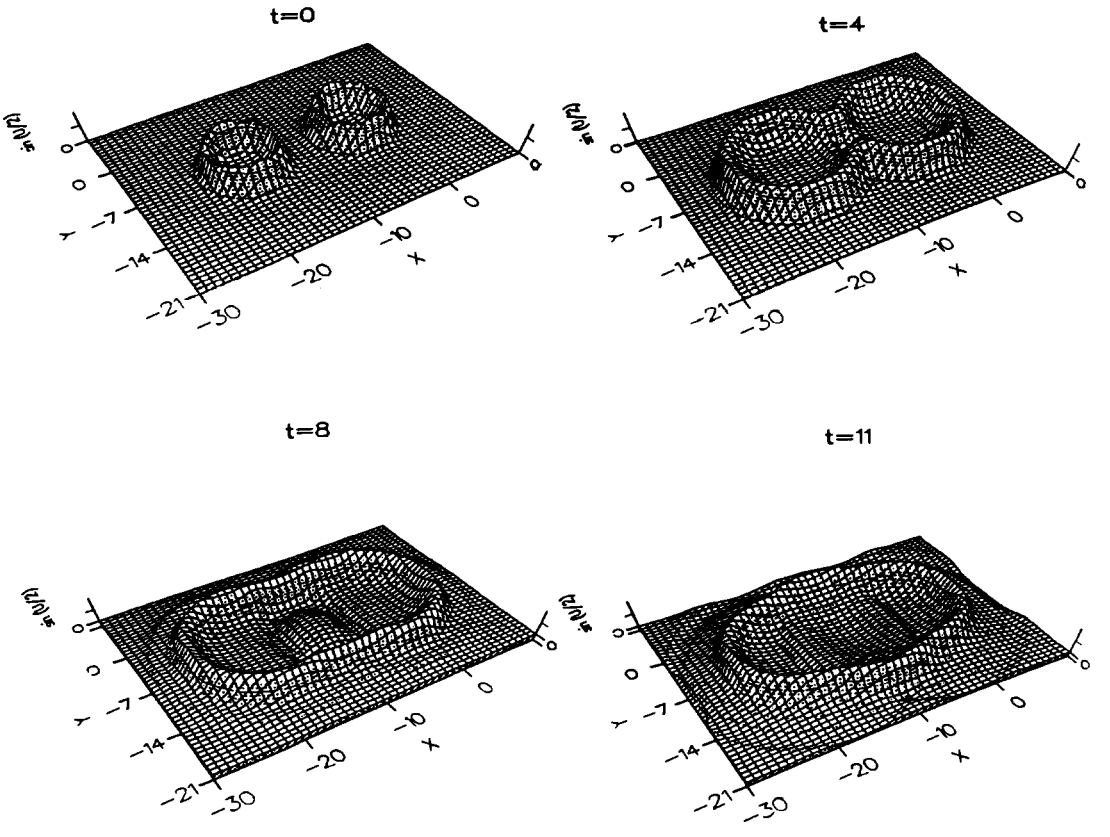

Fig. 6.

6.3.2. *Collision of two circular ring solitons*

The collision between two circular solitons is considered for $F(x, y) = 1$ and initial conditions

$$f(x,y) = 4\tan^{-1}\exp\left((4 - \sqrt{(x+3)^2 + (y+7)^2}/0.436\right), \quad -10 \leqslant x \leqslant 10, \quad -7 \leqslant y \leqslant 7 \tag{6.19}$$

$$g(x,y) = 4.13\operatorname{sech}\left((4 - \sqrt{(x+3)^2 + (y+7)^2}/0.436\right), \quad -10 \leqslant x \leqslant 10, \quad -7 \leqslant y \leqslant 7 \tag{6.20}$$

over the region $-10 \leqslant x \leqslant 10$, $-7 \leqslant y \leqslant 7$ and are presented in Fig. 6 for $\beta = 0.05$ at $t = 4$, 8 and 11 in terms of $\sin(u/2)$. The solution is extended across $x = -10$ and $y = -7$ by symmetry relations. The results in Fig. 6 show the collision between two expanding circular ring solitons in which, as a result of the collision, two oval-ring solitons bounding an annular region emerge into a larger oval ring soliton. For a large value of β, it is found that the dissipative term is slowing down the two initial ring solitons to emerge into a larger oval ring soliton. For example, with $\beta = 5$ the two ring solitons at time $t = 11$ still look like those given at $t = 1.5$ for $\beta = 0.05$.

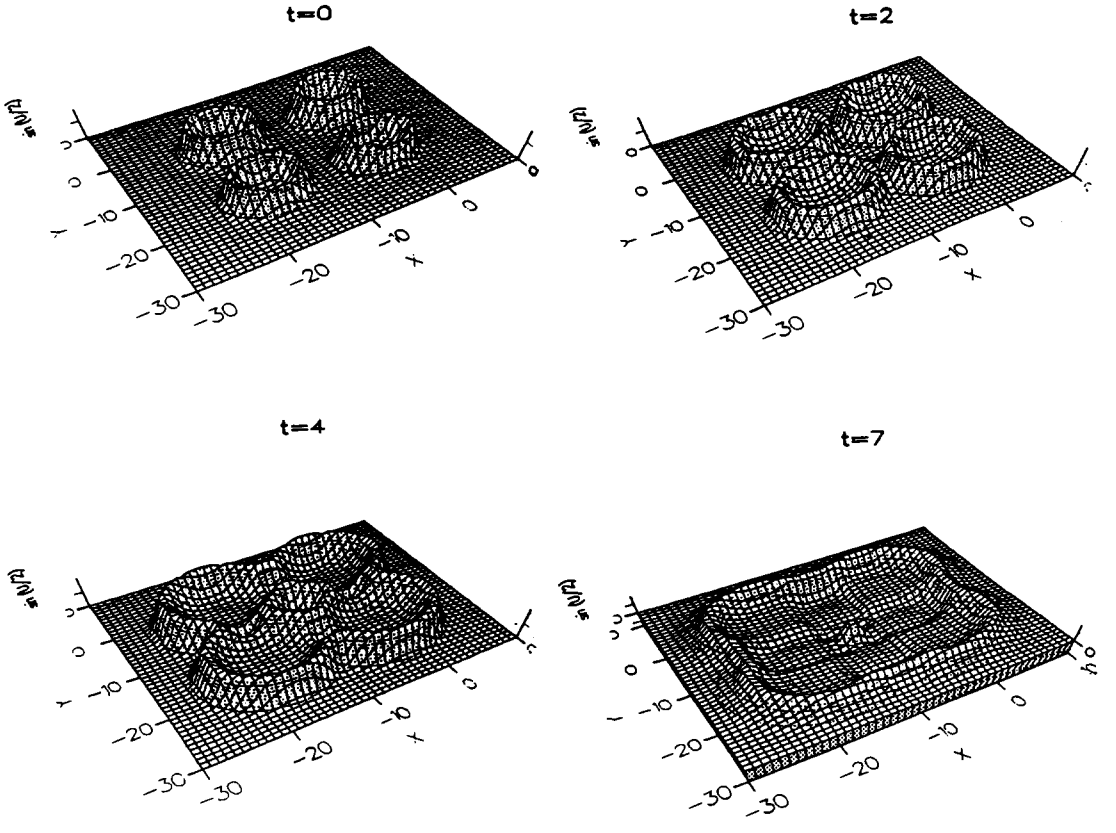

Fig. 7.

6.3.3. Collision of four circular ring solitons

Finally, a collision of four expanding circular ring solitons is investigated for $F(x,y) = 1$ and initial conditions

$$f(x,y) = 4\tan^{-1}\exp\left((4-\sqrt{(x+3)^2+(y+3)^2}/0.436\right), \quad -30 \leqslant x,y \leqslant 10 \tag{6.21}$$

$$g(x,y) = 4.13\cosh\left((4-\sqrt{(x+3)^2+(y+3)^2}/0.436\right), \quad -30 \leqslant x,y \leqslant 10 \tag{6.22}$$

over the domain $-30 \leqslant x,y \leqslant 10$. The solution was found over one-quarter of the domain and then it was extended across $x = -10$ and $y = -10$ by symmetry relations. The results are depicted in Fig. 7 for $\beta = 0.05$ at $t = 2$, 4, 6 and 7 in terms of $\sin(u/2)$, from which observations similar to those related to the collision of two expanding circular ring solitons may be made.

7. Concluding Remarks

A numerical method arising from a two-step, one-parameter method has been developed for the numerical solution of a damped Sine-Gordon equation.

Numerical experiments for various cases involving line and ring solitons are reported. For a small value of β, it was found that the effect of the dissipative term in the solutions of the Sine-Gordon equation is small in comparison with the undamped Sine-Gordon equation, whereas for a large value of β, the dissipative term was found to slow down the evolution of the line and ring solitons from their initial position as time increases.

For $\beta = 0.05$, results like 4π-break up into 2π kinks, which move away from each other undisturbed were found for the superposition of line solitons. Two symmetric dents are found to move towards each other and to retain their shape after the collision for the perturbed single line soliton. For the line soliton in an inhomogeneous medium, it was found that the line is transmitted across the inhomogeneity almost as a straight line soliton.

Shrinking phase initially, oscillating behaviour, and a forming of a ring soliton again are observed for the circular ring soliton. Finally, for the collision between two circular ring solitons, expanding ring solitons and emergence into a larger oval ring-soliton are observed. Similar observations can be made also for the collision of four circular ring solitons.

Finally, it was seen that, for the case where the exact solution is known, the global extrapolation involving both space and time produced noticeable reductions in error. These results supported the confidence in applying this method to problem (2.1) in which the theoretical solution is not known.

Solutions to the Sine-Gordon equation were found to exhibit little numerical dispersion for values of the space and time steps within the scheme's stability range.

The authors are very grateful to the referees for their valuable comments and suggestions, which have improved the paper.

References

1. R.K. Dodd, J.C. Eilbeck, J.D. Gibbons and H.C. Morris, *Solitons and Nonlinear Wave Equations*. London Academic Press (1982).
2. P.G. Drazin and R.S. Johnson, *Solitons: An Introduction*. University Press, Cambridge (1989).
3. J.D. Josephson, Supercurrents through barriers, *Advances in Physics* 14 (1965) 419–451.
4. P.L. Christiansen and P.S. Lomdahl, Numerical solution of 2 + 1 dimensional Sine-Gordon solitons. *Physica* 2D (1981) 482–494.
5. R. Hirota, Exact three-soliton solution of the two-dimensional Sine-Gordon equation. *J. Phys. Soc. Japan* 35 (1973) 1566.
6. J. Zagrodzinsky, Particular solutions of the Sine-Gordon equation in 2 + 1 dimensions. *Phys. Lett.* 72A (1979) 284–286.
7. P.L. Christiansen, and O.H. Olsen, Ring-shaped quasi-soliton solutions to the two and three-dimensional Sine-Gordon equations. *Physica Scripta* 20 (1979) 531–538.
8. G. Leibbrandt, New exact solutions of the classical Sine-Gordon equation in 2 + 1 and 3 + 1 dimensions. *Phys. Rev. Lett.* 41 (1978) 435–438.
9. P. Kaliappan and M. Lakhshmanan, Kadomtsev-Petviashvili, two dimensional Sine-Gordon equations: reduction to Painleve transcendents. *J. Phys. A.: Math. Gen.* 12 (1979) L249–L252.
10. J. Argyris, M. Haase and J.C. Heinrich, Finite element approximation to two-dimensional Sine-Gordon solitons. *Computer Methods in Applied Mechanics and Engineering* 86 (1991) 1–26.
11. K. Nakajima, Y. Onodera, T. Nakamura and R. Sato, Numerical analysis of vortex motion on Josephson structures. *Journal of Applied Physics* 45(9) (1974) 4095–4099.
12. B.A. Malomed, Dynamics of quasi-one-dimensional kinks in the two dimensional Sine-Gordon model. *Physica D*, 52 (1991) 157–170.
13. I.S. Greig and J. Ll. Morris, A Hopscotch method for the Korteweg-de Vries equation. *J. Comput. Phys.* 20 (1976) 64–80.

14. E.H. Twizell, Y. Wang and W.G. Price, Chaos-free numerical solutions of reaction-diffusion equations. *Proc. R. Soc. Lond.* A 430 (1991) 541–576.
15. J.D. Lambert, *Numerical Methods for Ordinary Differential Systems: The Initial Value Problem.* John Wiley and Sons 1991.
16. Y.I. Shokin, Springer-Verlag, Berlin, Heidelberg, *The Method of Differential Approximation.* New York (1983).
17. E. Turkel, Phase error and stability of second order methods for hyperbolic problems. *J. Comput. Phys.* 15 (1974) 226–250.